COMPACT X-RAY FREE ELECTRON LASE BASED ON AN OPTICAL UNDULATOR

C. Maroli, V. Petrillo, Dipartimento di Fisica dell'Università di Milano-INFN Sezione di Milano Via Caloria,16, 20133 Milano, Italy
L. Serafini, A. Bacci, A Rossi, P. Tomassini, *INFN*-Sezione di Milano, Via Celoria,16, 20133 Milano, Italy

Abstract

The interaction between a very high-brilliance electron beams and a relativistically intense counter-propagating laser pulses produces X rays via FEL collective amplification. The phenomenon is, however, very selective, so that the characteristics of both electron and laser beam must satisfy tight requirements in terms of beam current, emittance, energy spread and laser amplitude stability within the pulse. The three dimensional equations governing the radiation phenomenon have been studied in both linear and non linear regime and solved numerically for the particular interesting values of wavelengths of 1 Ang, 1nm and 12 nm. The performance of the collective Thomson source has been compared with that of an equivalent static undulator.

INTRODUCTION

The collective effects that develop in the classical Thomson back-scattering give rise to intense X-ray pulses easily tunable and highly monochromatic at a level a few orders of magnitude larger than the incoherent radiation. Due to recent technological developments in the production of high brilliance electron beams and high power CPA laser pulses, it is now even conceivable to make steps toward their practical realisation.

The phenomenon of the impact between the electron beam and the laser pulse has characteristics similar to the free electron laser and has been studied in previous papers[1-2]. The lasing is rather difficult to start up and the power saturation level is lower than that achieved in conventional static wigglers. It is however large enough to be interesting for application as fast probing for chemical process, monochromatic X imaging, phase contrast imaging, deep probing for inertial fusion research, considering moreover the fact that this kind of set-up is compact and considerably less expensive than static FEL.

In this paper we present several details about this X-ray production phenomenon, analysing various beam lines producing different electron bunches as well as various situations relevant to the synchronization between the electron beam and the laser pulse. Finally, we have compared the results of the radiation levels obtained with our 'ad hoc' radiation code EURA (for Electromagnetic Undulator Radiation Analysis) with those provided by the code GENESIS 1.3 currently used in FEL simulations [3], which is however not presently able to model electro-magnetic undulators. The answers given by both codes are qualitatively similar and also the quantitative estimates of saturation power and gain length are very close, when magnetostatic undulators are considered.

NUMERICAL SOLUTION OF 3D EQUATIONS

We have first studied the use of a CO_2 laser of wavelength λ_L=10 micron. High power lasers of this frequency are characterized by 70-100 GW of power and up to 300 psec of time pulse length.

By fixing the mean energy of the electron beam around the value <E>=30 MeV, i.e. <γ>=60, using the resonance condition for the back-scattering Thomson, $\lambda_R=\lambda_L(1+a_{L0}^2)/4\gamma^2$ and assuming the laser parameter $a_{L0}\leq 0,5$, X rays of wavelengths λ_R of the order of 7-9 Angstrom can be obtained. For this case, collective effects and FEL instability develop when the beam transverse normalized emittance does not exceed the value ε_x=0.5, and if the energy spread $\Delta\gamma/\gamma$ is contained in few 10^{-4}. Values of this kind are out of the current state-of-the-art of high–brightness beams but represent an interesting challenge for a possible future operation scenario.

Our numerical simulations for the case of the electromagnetic undulator have been performed with the 3D code EURA, which is a three-dimensional, time dependent code that integrates equations (2-5) using a forth order Runge-Kutta method for the particles and an explicit finite difference scheme for the radiation equation. The bunching factor is calculated along the beam by selecting, around each point, a moving portion of the bunch including several buckets.

The data obtained with EURA for a static undulator have been compared with similar data produced with the code GENESIS 1.3 widely used in the FEL analysis. The comparison is presented in Fig 3 where data from EURA (black curve (b)) and from GENESIS 1.3 time dependent (red curve (a)) are reported.

The data chosen for the comparison are: undulator parameter a_w=0.3, undulator period λ_w=10µm, radiation wavelength λ_R=1.515 nm, ε_x=0.3 mm mrad, r.m.s. transverse dimension σ_x=12.5 µm (corresponding to a maximum radius of 25 μm), a constant external magnetic field. EURA simulates the entire bunch, which has been taken 1 mm long, while GENESIS 1.3 simulates a fraction of N=1000 slices of width λ_R, separated by $z_{sep}=N_{sep}\lambda_R$ with $N_{sep}=20$, corresponding to approximately 75 cooperation lengths.

We note that in both simulations with EURA and GENESIS 1.3 it is very important to set the correct detuning with respect to the nominal resonance frequency, because otherwise the growth of the instability is strongly damped. The computed gain lengths are of L_g =3,6 mm for EURA and L_g =4.08 mm for GENESIS 1.3, while the analytical expressions by Ming Xie [3] give

$$L_g=L_{1D}(1+\eta) \qquad (1)$$

with L_{1D}, the one-dimensional gain length, estimated numerically as about 1.97 mm,

$$\eta=(0.45\eta_d^{0.57}+0.55\eta_\varepsilon^{1.6}+3\eta_\gamma^{2}+\ldots) \qquad (2)$$

and:

$$\eta_d=L_{1D}\lambda_R/(4\pi\sigma_x^2) \qquad (3)$$

$$\eta_\varepsilon= L_{1D}2\pi\varepsilon_{,x}^2 \;/(\gamma^2\sigma_x^2\lambda_R) \qquad (4)$$

$$\eta_\gamma= 4\pi\, L_{1D}(\delta\gamma/\gamma)/\lambda_w \;. \qquad (5)$$

It can be seen that for the case analysed η_d is about 1,5 10^{-3} , η_γ=0.24, negligible respect to η_ε which in this case can be evaluated through (24) as η_ε =1.31 yielding on the whole to L_g =3,96 mm.

As shown in fig 3, EURA gives a gain length slightly shorter than GENESIS 1.3, with a faster saturation, but at a smaller power level. Other characteristics are an initial growth in the first gain length less steep and stronger post-saturation power oscillations due probably to a deeper entrapment of the particles. A zero-order comparison on the time independent behaviour is impossible, because EURA is, for its nature, only time dependent. The scenario is similar to that pointed out in the GENESIS 1.3 versus GINGER comparison [4,5]. Other data relevant to the analysis made with GENESIS 1.3 are reported in Fig 2 where the signal on the bunch at z=3 cm is presented.

In fig 3 the radiation obtained with a conventional static undulator (already presented in fig 3) has been plotted together with the case of an electromagnetic wiggler of equal intensity and wavelength, in the case of $a_w=a_{L0}=0.3$, $\lambda_w=\lambda_L=10$ μm, $\varepsilon_x=0.3$ mm mrad, $\sigma_x=12.5$ μm (corresponding to a maximum radius of 25 μm).The differences introduced by the resonance condition lead, however, to a radiation wavelength smaller than a factor of two respect to the static undulator, so that, for the electromagnetic undulator, $\lambda_R=0.7578$ nm. The simulations show that the electromagnetic undulator produces a power saturation value of 1.93 MW in less than 2.5 cm, with an average gain length of about 1.8 mm, while the static undulator reaches 1.33 MW of power in about 3 cm, with a gain length near to 3.5 mm.

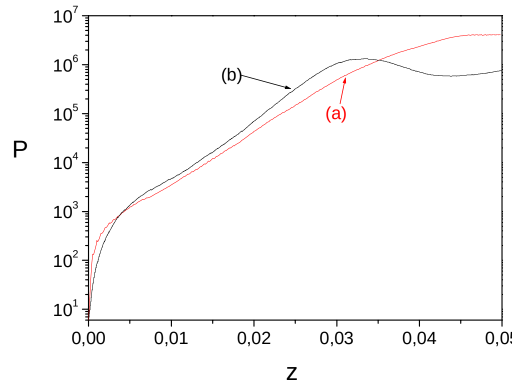

Fig 1: Radiated power P in Watt versus z coordinate in meter for (a) simulations made with GENESIS 1.3 and (b) with EURA for $a_w=0.3$, $\lambda_w=10$ μm, $\lambda_R=1.515$ nm, $\varepsilon_x=0.3$ mm mrad, $\sigma_x=12.5$ μm (corresponding to a maximum radius of 25 μm), a constant external static magnetic field.

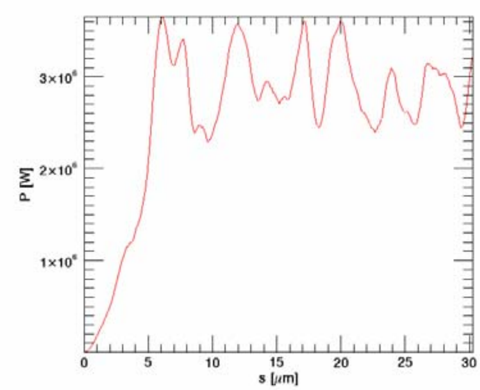

Fig 2: Radiated power P (in Watt) versus the coordinate along the bunch s (in microns) at z=3 cm and for the same case as fig 5. Simulation made with GENESIS 1.3

In fig 4 a case analogous to fig 3 is presented, but the emittance value, that in this case has been increased to 0.6. In this case the power level achieved by electromagnetic and static undulators are respectively 0.36 MW and 0.26 MW, with gain lengths of respectively 2.9 and 5.08 mm. In Fig 5 a summary of data is presented showing the gain lengths ((a) and (b)) deduced by a fitting of the numeral data (on the left scale) and the saturation radiation intensity ((c) and (d)) (on the right scale) for both electromagnetic (in blue) and static (in black) undulators. A case particularly important for its applications is the production of radiation characterized by wavelength λ_R of about 1 Angstrom. . This value can be reached with a Ti:Sa laser with $\lambda_L=0.8$ μm, $a_{L0}=0.8$, $\langle\gamma\rangle=55$, $L_b=300$ μm, $r_b=7$ μm, a total charge of 3 nC, for a current of 3 KA.

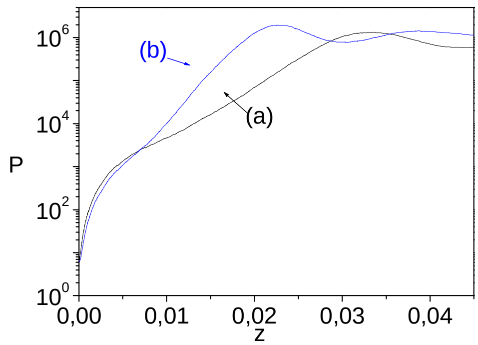

Fig 3: Radiated power P (in Watt) vs z (in meter) for (a) static undulator and (b) electromagnetic undulator. a_w=0.3, λ_w=10 μm, ε_x=0.3 mm mrad, σ_x=12.5 μm (corresponding to a maximum radius of 25 μm).For the static undulator λ_R =1.515 nm, while for the e.m. undulator λ_R =0.7578.

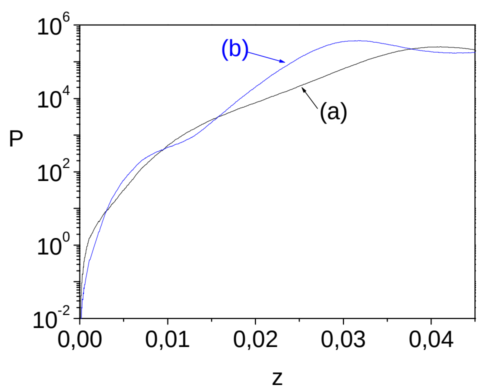

Fig 4: Same as Fig 3 but with ε_x=0.6 mm mrad.

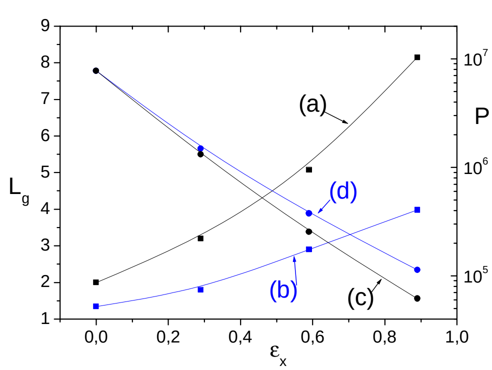

Fig 5: Gain length L_g in mm (left scale) versus ε_x in mmmrad. Radiation power P (in Watt) versus ε_x in mmmrad on the right scale for a_w=0.3, λ_w=10 μm, σ_x=12.5 μm (corresponding to a maximum radius of 25 μm). (a) and (c) refer to a static undulator case, while (b) and (d) to an electromagnetic one.

Cases with emittance ε_x=0.26 mm mrad (curve (a)) ε_x =0.54 mm mrad (curve (b)) and ε_x =0.8 mm mrad (curve (c)) are presented in Fig 6, where the power obtained in Watt is plotted versus z (in meter).

The factor $\rho = \frac{1}{\gamma}\left(\frac{\omega_b^2 \bar{a}_{L0}^2}{16\omega_L^2}\right)^{\frac{1}{3}}$ (ω_b being the plasma frequency of the beam and ω_L the laser frequency) is 4.17 10^{-4} and the radiation wavelength is λ_R =1.13 A. In this case we are at the limit of validity of the classical model, because the quantum factor q is 0.9, and quantum effects, arising when q>1, can play an important role [7,8]. However, the previous condition on q relies on one-dimensional models. Three-dimensional considerations [9] seem to point out a relaxation of the above condition due to the enlargement of the bandwidth associated to non-ideal and geometrical effects so that the requirement q>1 should be rather replaced by $q\rho > \max(\rho, \Delta\gamma/\gamma, \varepsilon_{n,x}^2/\sigma_x^2)$, where $q\rho$ is the relative energy separation between the quantum lines, ρ is the one-dimensional natural bandwidth and $\Delta\gamma/\gamma$ and $\varepsilon_{n,x}^2/\sigma_x^2$ are respectively the inhomogeneous line broadening due to energy spread and emittance effects [10]. In our case we have $q\rho$=4 10^{-4}, but for the case (a) $\varepsilon_{n,x}^2/\sigma_x^2$ does never go under 7 10^{-4}. The cases with larger emittance are, in this sense, even less critical respect to the presence of quantum effects. The cases presented require an amount of laser power outside the present status of the art, but achievable in the near future [11]. In fact, for instance, in the case (b) with emittance ε_x =0.54 mm mrad, at saturation the beam has a maximum radius of about 15 μm; assuming for the laser in the waist a spot size of 20 μm, we obtain the needed laser power of more than 17 TW for at least 1.5 mm, corresponding to a total laser energy of about 85 J.

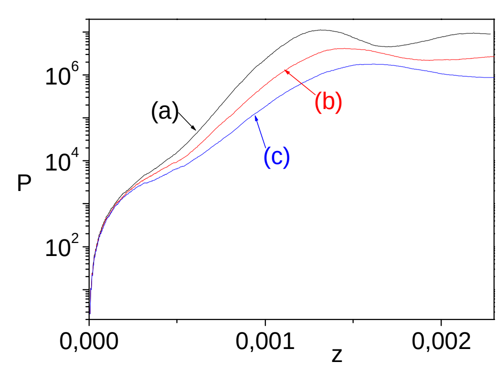

Fig 6: Radiated power P (in Watt) vs z (in meter) for an electromagnetic undulator. a_{L0}=0.8, λ_L=0.8 μm, σ_x=3.5 μm, (corresponding to a maximum radius of 7 μm), $\Delta\gamma/\gamma=10^{-4}$, λ_R=1.13 Angstrom. (a) ε_x=0.26 mm mrad .(b) ε_x=0.54 mm mrad (c) ε_x=0.8 mm mrad.

Also the properties of the electron beam are extreme, due to the required condition of large current, low emittance, minimum energy spread, high focusing and relatively small γ.

A case equally interesting, but less difficult to realise is a radiation wavelength of about 1 nm. In addition to the case presented in the previous paragraph relying on the use of the CO_2 laser (characterized by a radiation wavelength λ_R of about 7.57 A), we present here the possibility of producing X-rays in the range of the nanometer with the Ti:Sa laser.

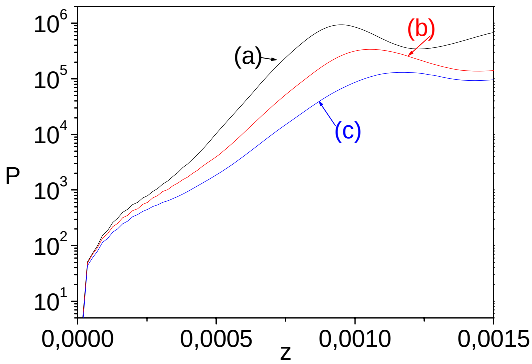

Fig 7 Radiated power P (in Watt) vs z (in meter) for an electromagnetic undulator. a_{L0}=0.8, λ_L=0.8 μm, σ_x=5 μm, (corresponding to a maximum radius of 10 μm), I=600 A, $\Delta\gamma/\gamma=10^{-4}$, λ_R=1.06 nm. (a) ε_x=0.26 mm mrad .(b) ε_x=0.54 mm mrad (c) ε_x=0.8 mm mrad..

In this case, in fact, the factor γ has been assumed γ=18.11 and a_{L0}=0.8, the resonant wavelength being about 1 nm. The total charge is Q=2 10^{-9} C, L_b=1 mm, so that the current I is I=600 A. Cases with different emittance are presented in Fig 11. The radiation power reaches 1 MW for the case with ε_x=0.26. The requirement of laser power can be evaluated by assuming a channel of 17 μm of maximum radius with a length of 1.1 mm for a power of 12 TW and a total energy of 48 J.

Finally, we present the possibility of producing 12 nm radiation by means of the CO_2 laser. For this case, the properties of the electron beam have been relaxed. In fact, we have assumed a γ of 16.5, a current of 150 A, an emittance of $\varepsilon_{,x}$=1.06 mm mrad , a maximum radius of 30 μm (σ_x=15. μm), an energy spread of 1.3 10^{-4}, conditions inside the present status of the art of the production of high brightness electron beams. The saturation value of the radiation power is very low, namely ten Kilowatt, but larger by a factor 20 than the incoherent radiation produced in the same bandwidth. The power saturation value can be considerably incremented up to 10 MW by shifting the focus of the beam. In Fig 8 the radiation power and the rms radius are presented for a_{L0}=0.5 and for the focus of the beam shifted at z=0.68 cm in correspondence of the middle of the exponentiation phase.

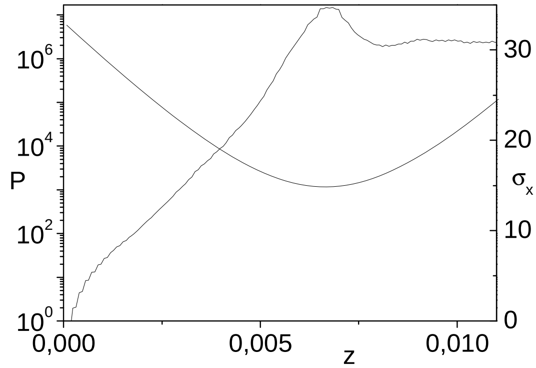

Fig 8: Left axis: radiated power P in Watt vs zin meter. Right axis: rms radius (in micron) vs z.

The laser power required is in this last case 100 GW with total energy 2.3 J, but considerable value of power radiation (namely P= 100 KW at 1 cm) can be reached also by limiting the laser parameter to a_{L0}=0.2, corresponding to 16 GW of laser power and 0.6 J of total energy.

REFERENCES

[1] A.Bacci, C. Maroli, V. Petrillo , L. Serafini: 'Eur. Phys. Jour. Appl. Phys', (2006), 2006080

[2] A.Bacci, M Ferrario, C. Maroli, V. Petrillo, L.Serafini: 'PRST AB',Vol.: 9 , (2006) 060704

[3]S. Reiche: Genesis 1.3 http:// pbpl.physics.ucla.edu/~reiche/

[4] Ming Xie, "Design Optimization for an X-Ray Free Electron Laser Driven by SLAC Linac," Proc. 1995 PAC, Dallas, May 1-5, 183.

[5] William M. Fawley, "A user manual for GINGER and its post-processor XPLOTGIN" (February 19, 2002). Lawrence Berkeley National Labora*tory*. Paper LBNL-49625. http://repositories.cdlib.org/lbnl/LBNL-49625

[6]W.M. Fawley: 'X-Ray FEL Simulation:Beam Modeling' ICFA 2003 Workshop on Start to end Numerical Simulations of X-RAY FEL's Fawley-ICFA03-Zeuthe..>http://citeseer.ist.psu.edu/xie95design.

[7] J.B. Murphy and C. Pellegrini: 'J Opt.Soc. Am. B'**,** Vol.: 2**,** (1985), pg.:259 .

[8] R. Bonifacio et al.: 'Nucl. Instrum. And Meth. A', Vol.: 543 ,(2005), pg.:645.

[9] Smetanin, I.V., Nakajima, K, Proceedings of the Second Symposium on Advanced Photon Research (JAERI-Con 2001-011) : 236-40, 2001

[10] Winthrop J. Brown and Frederic V. Hartemann: 'Phys.Rev. ST A B', Vol.:7 (2004), 060703.

[11] M. D. Perry et al., "Petawatt Laser Pulses," Optics Letters, Vol. 24 (1999), p. 160, E. Hugonnot, J. Luce, and H. Coïc, "Optical parametric chirped-pulse amplifier and spatiotemporal shaping for a petawatt laser", Appl. Opt. 45, 377-382 (2006)